MEGAWATT, PULSED ULTRAVIOLET PHOTON SOURCES FOR MICROBIAL INACTIVATION

Patrick Hancock[1], Randy Curry and Kenneth McDonald
University of Missouri-Columbia
Department of Electrical Engineering
Columbia, Missouri 65211
curryrd@missouri.edu

Larry Altgilbers
United States Army Space and Missile Defense Command
Huntsville, Alabama 35805

Abstract

The University of Missouri-Columbia (UM-C) has developed pulsed ultraviolet (UV) photon sources commensurate with enhanced ultraviolet inactivation of hazardous microbials on surfaces or in a water matrix. Pulsed xenon flashlamps have been optimized to produce a high ultraviolet photon yield in the 180 – 320 nm range that is lethal to microbials; and has a high cross-section interaction with photosensitizer chemicals to synergistically enhance microbial inactivation. Electrical models have been derived to predict the time dependent plasma discharge impedance profiles of the flashlamp UV source. These models are discussed in the following paper.

I. INTRODUCTION

Researchers at the University of Missouri – Columbia, have developed a rapid process to inactivate pathogenic microorganisms resident on surfaces by misting photosensitizing chemical solutions onto the surfaces and illuminating them with ultraviolet (UV) light. This process relies heavily on the UV spectrum below 280 nm (UV-C) for these energetic wavelengths directly damage cellular DNA and have a high cross-section interaction with the photosensitizer chemicals, yielding radicals and reactive oxidative species that synergistically enhance microbial kill [1]. Accordingly, a high power linear, xenon flashlamp system has been developed to support this research effort. Spectra from the flashlamp is emitted as atomic transition line radiation superimposed on a broadband continuum, ranging from the deep UV into the infared. Xenon gas was chosen for it's high efficiency of electrical to optical energy conversion, particularly in the UV-C band of interest [2]. The flashlamp system was optimized for UV-C generation through circuit design [3-7], lamp selection, and short pulse operation [8,9]. It has been shown that the current density has a substantial effect on tailoring the spectral output of the xenon discharge. As this parameter is increased from a few hundred to a few thousand A/cm2; continuum radiation intensity increases rapidly, the average spectrum shifts toward shorter wavelengths, and the average photon energy is increased [2,10].

II. METHODS AND MATERIALS

A Perkin Elmer linear xenon flashlamp, described in Table 1, was driven from a critically damped single stage pulse forming network (PFN) consisting of a 32 μF capacitor and a 1.4 μH inductor.

Table 1. Perkin Elmer flashlamp properties.

Flashlamp model	Fill pressure	Arc length	Bore diameter
L8083E	450 torr Xe	10 cm	0.7 cm

A diode stack in parallel with the flashlamp provided reverse current protection. An external trigger circuit based on a Perkin Elmer TR180B trigger transformer was utilized to initiate ionization within the flashlamp. Electrical discharge energies ranging from 16 - 100 Joules per pulse resulted in current pulse widths from approximately 23.3 to 15.5 μs respectively. Figure 1 details the PFN driving circuit and external trigger circuit configurations used.

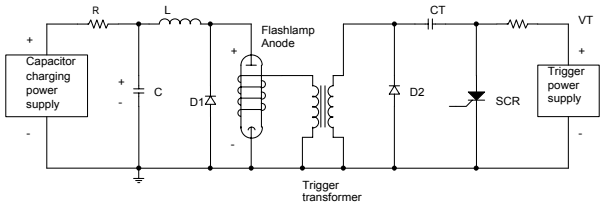

Figure 1. PFN and external trigger circuit configuration.

A flashlamp simulation model, graphically illustrated in figure 2, was developed for the Pspice circuit

[1] Currently with Honeywell Kansas City Plant

Report Documentation Page

Form Approved
OMB No. 0704-0188

1. REPORT DATE	2. REPORT TYPE	3. DATES COVERED
JUN 2003	**N/A**	**-**

4. TITLE AND SUBTITLE	5a. CONTRACT NUMBER
Megawatt, Pulsed Ultraviolet Photon Sources For Microbial Inactivation	5b. GRANT NUMBER
	5c. PROGRAM ELEMENT NUMBER
6. AUTHOR(S)	5d. PROJECT NUMBER
	5e. TASK NUMBER
	5f. WORK UNIT NUMBER
7. PERFORMING ORGANIZATION NAME(S) AND ADDRESS(ES) **University of Missouri-Columbia Department of Electrical Engineering Columbia, Missouri 65211**	8. PERFORMING ORGANIZATION REPORT NUMBER
9. SPONSORING/MONITORING AGENCY NAME(S) AND ADDRESS(ES)	10. SPONSOR/MONITOR'S ACRONYM(S)
	11. SPONSOR/MONITOR'S REPORT NUMBER(S)

12. DISTRIBUTION/AVAILABILITY STATEMENT
Approved for public release, distribution unlimited

13. SUPPLEMENTARY NOTES
See also ADM002371. 2013 IEEE Pulsed Power Conference, Digest of Technical Papers 1976-2013, and Abstracts of the 2013 IEEE International Conference on Plasma Science. IEEE International Pulsed Power Conference (19th). Held in San Francisco, CA on 16-21 June 2013. U.S. Government or Federal Purpose Rights License., The original document contains color images.

14. ABSTRACT
The University of Missouri-Columbia (UM-C) has developed pulsed ultraviolet (UV) photon sources commensurate with enhanced ultraviolet inactivation of hazardous microbials on surfaces or in a water matrix. Pulsed xenon flashlamps have been optimized to produce a high ultraviolet photon yield in the 180 320 nm range that is lethal to microbials; and has a high cross-section interaction with photosensitizer chemicals to synergistically enhance microbial inactivation. Electrical models have been derived to predict the time dependent plasma discharge impedance profiles of the flashlamp UV source. These models are discussed in the following paper.

15. SUBJECT TERMS

16. SECURITY CLASSIFICATION OF:			17. LIMITATION OF ABSTRACT	18. NUMBER OF PAGES	19a. NAME OF RESPONSIBLE PERSON
a. REPORT	b. ABSTRACT	c. THIS PAGE			
unclassified	**unclassified**	**unclassified**	**SAR**	**4**	

simulation software package. The model simulates the behavior of the plasma for a given set of discharge parameters determined by the PFN circuit components and the flashlamp physical properties. The discharge is characterized by the plasma resistivity, plasma temperature, and plasma resistance, pursuant to the following equations [7,11]:

$$\rho = 0.96x10^{4}\left(T\right)^{-3/2} \qquad [1]$$

$$T = 519\left(j\sqrt{r}\right)^{4/11} \qquad [2]$$

$$R = \rho l / A \qquad [3]$$

where T = Plasma temperature (^{o}K)
j = Current density (A/cm^2)
r = Plasma radius (cm)
ρ = Plasma resistivity (Ω-cm)
R = Plasma resistance (Ω)
l = Flashlamp arc length (cm)
A = Flashlamp area (cm^2)

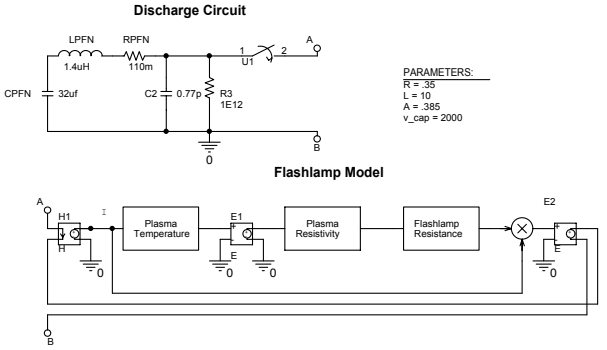

Figure 2. Flashlamp simulation model.

Equations 1, 2, and 3 are the culmination of an extensive literature review of xenon arc characteristics. Equation 1 was derived from Spitzer's resistivity theory for a fully ionized (Lorentzian) plasma [12].

A current controlled voltage source (H1) and two voltage controlled voltage sources (E1, E2) are used simply as buffers in the model (figure 2). Current generated in the discharge circuit is transformed into an equivalent voltage at nodes A and B of the flashlamp model, and is used as input to the calculation (ABM) blocks. Equations 1, 2, and 3 are then utilized in combination to determine the plasma temperature based on the discharge current density, the plasma resistivity as a function of the plasma temperature, and finally the plasma resistance. The multiplier block located between the flashlamp resistance block and E5 part is used to develop the voltage across the flashlamp and feed it back to nodes A and B by multiplying the input current and the time varying resistance of the flashlamp. The parameter block is used for ease in manipulating flashlamp parameters (i.e. arc length, bore diameter and cross sectional area) allowing a variety of lamps styles to be simulated. The model assumes a fully ionized quasi-collisionless plasma which completely fills the flashlamp bore. Future improvements to the model will incorporate the temporal behavior of the lamp inductance and resistance.

The dose or energy per unit area ultraviolet light calibration was measured utilizing a model S310 Scientech VectorTM laser power meter and an AstralTM model AC25HD Calorimeter. Cut-on filters, coupled with a subtraction method, were employed to characterize the spectral output for the flashlamp. A family of high quality Andover cut-on filters was selected for their sharp wavelength cut-on properties. Corrections were made for both the calorimeter response (~92%) and filter response (~90%) from 180 nm to 2.1 μm. Radiant energy measurements were made with the calorimeter placed 30 cm from the flashlamp, which was mounted within a parabolic reflector housing to optimize radiant energy on target. The lamp was typically operated at a pulsed repetition rate of 10 Hz, and the calorimeter was operated in an average power mode over a 60 to 90 second time period to minimize the effect of pulse-to-pulse variations in output radiation. The spectrum was obtained with a Princeton Instruments Optical Multichannel Analyzer. Corrections for both the wavelength dependent response of the detector and grating efficiency were included. The measurements were used to validate the model.

III. EXPERIMENTAL RESULTS

Figures 3 and 4 clearly demonstrate the rapid increase in continuum radiation, particularly in the 200 nm to 400 nm regions, manifest to increasing discharge energy and current density. The increase in discharge energy between figures 3 and 4 is 300% resulting in a current density increase of 270%.

As shown in figure 5, nearly 50% of the total optical energy being radiated between 200 nm and 600 nm falls in the UV wavelength band. Electrical to optical energy conversion efficiency over a wavelength range of 180 nm to 2.7 μm was found to be as high as 73% for 64 J and 100 J discharges. PFN circuit efficiency was accounted for in determining percentage of the energy actually delivered to the flashlamp. While the observed conversion efficacy is high, it is not unprecedented, as others researchers have measured conversion efficiencies of 65% from 350 nm to 1.1 μm [10], and 78% for UV through IR wavelengths [13].

Figure 6 shows the relative percentages of UV and UV-C emission for 16 J through 64 J discharges. The data shows that the percent increase in UV radiation is 47.4% while the percent UV-C emission increases nearly twice

as fast at 96.1% as a function of discharge energy density. A similar plot of this data is derived as a function of percent explosion energy, or the ratio of input energy to single shot explosion energy of the flashlamp. This parameter is defined as the input energy likely to result in rapid envelope failure, and is a function of lamp dimensions and fill pressure.

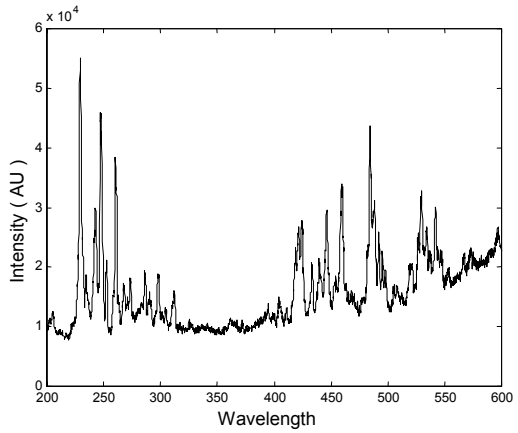

Figure 3. Xenon spectra for a 16-Joule discharge

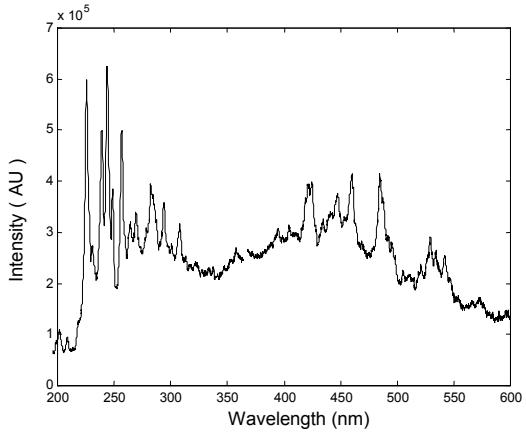

Figure 4. Xenon spectra for a 100-Joule discharge.

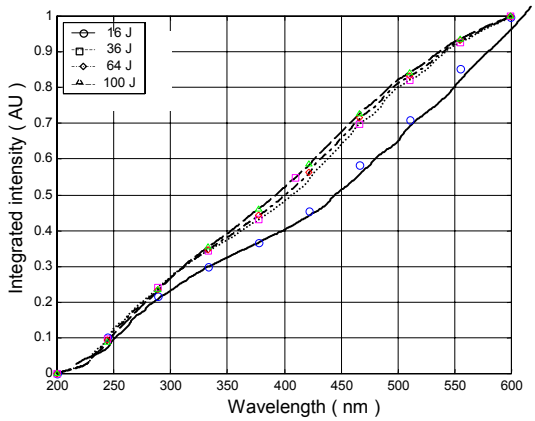

Figure 5. Integrated spectral emission for increasing discharge energy.

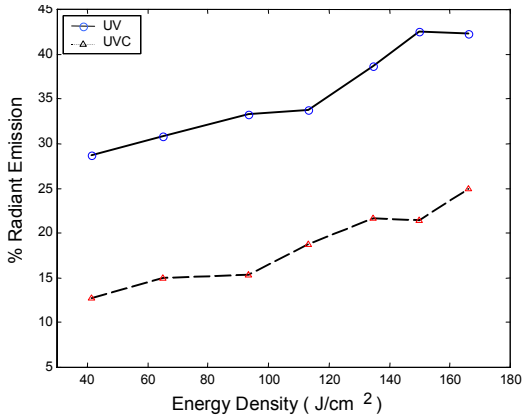

Figure 6. Percent ultraviolet emission as a function of discharge energy density.

IV. DISCUSSION

The measured flashlamp characteristics were compared to selected simulation results obtained with two PFN circuit inductances as shown in figures 7-9. This is meant to illustrate the effect of a time variant flashlamp arc inductance, which is not incorporated in the current flashlamp simulation model. Hohlfeld gives a review of this subject [6,11]. This effect, which becomes more prominent for larger lamps and longer pulse durations, is a function of the time varying plasma arc diameter and flashlamp energy deposition. At early times in the discharge when the plasma arc is growing, the effective lamp inductance is higher than when the arc has fully developed. This effect may be seen in the current plot of figure 7 for a 36 J discharge. Current rise-time is more accurately simulated with the higher inductance value. The higher inductance tends to slow current rise-time and a decrease in the peak current discharge current. The opposite effect is seen in the current fall-time when the arc is fully developed and inductance is lowered. In this case the lower discharge circuit inductance is a better approximation to actual flashlamp behavior.

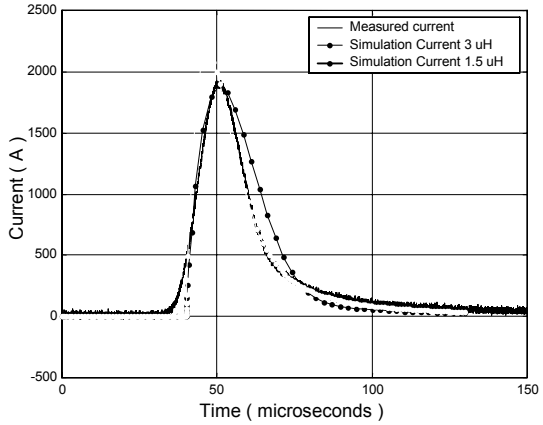

Figure 7. Measured and simulated flashlamp current

The same effect is manifest in the measured vs. modeled lamp resistance, as shown in figure 8. The resistance is equal to the measured voltage drop across the lamp divided by the current. The resistance was typically on the order of 200 - 400 mΩ during the high current phase of operation.

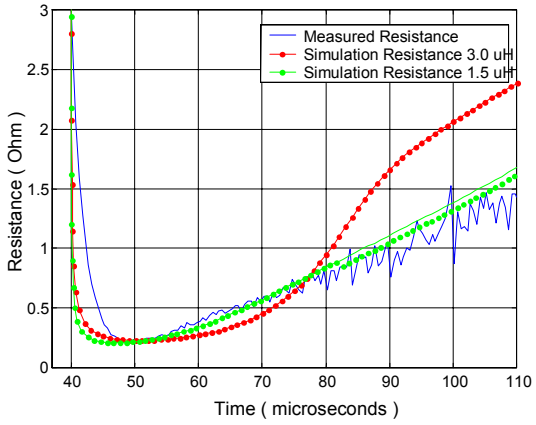

Figure 8. Measured and simulated flashlamp resistance.

The model developed using the Spitzer equation and the Gonz relationship when integrated with a circuit simulation program predict the measured flashlamp plasma profile and resistance. It is our intent to further expand this model to include a time varying inductance that includes the time dependent expansion rate of the flashlamp plasma. In reality this may be somewhat difficult for the plasma initiates at the surface of the flashlamp bore, and then rapidly expands to fill the bore of the lamp. The initial characteristics of the flashlamp plasma are however strongly dependent on the trigger voltage and waveform. As such the time dependent variation of inductance with current risetime may be difficult to model and scale to various bore diameters or current densities.

V. ACKNOWLEDGEMENTS

This work has been supported by the US Marine Corp. (MarCorSysCom), CBIRF, and the US Army Space and Missile Defense Command, under contract No. C-5-34220. We wish to thank Phil Abel, and Kris Coats, for their technical assistance.

VI. REFERENCES

[1] K.F. McDonald, et al, ”Comparison of Pulsed and CW Ultraviolet Sources to Inactivate Spores on Surfaces.” 13th IEEE International Pulsed Power Conference, pgs 604-607, Las Vegas Nevada, 2001.

[2] J.R. Oliver and F.S. Barns, "A Comparison of Rare-Gas Flashlamps," IEEE Journal of Quantum Electronics, vol. QE-5, pp. 232-237, May, 1969.

[3] A.D. McLeod. *Design Considerations for Triggering Of Flashamps*, 1997. (UnPub)

[4] ILC, "High Performance Flash and Arc Lamps," *ILC Q-Arc Flashlamp Data Book*, vol. 3, 1987.

[5] J.P. Markiewicz and J.L. Emmitt, "Design of Flashlamp Driving Circuits," *Journal of Quantum Electronics*, vol. QE, pp. 707Nov, 1966.

[6] R.G. Hohlfeld, W. Manning, and D.A. MacLennan, "Self-inductance effects in linear flashtubes: an extension to the Markiewicz and Emmett theory," *Applied Optics*, vol. 22, pp. 1986-1991, Jul 1, 1983.

[7] T. Efthymiopoulos and B.K. Garside, "High-Energy short-pulse flashlamps: operating characteristics," *Applied Optics*, vol. 16, pp. 70-76, Jan, 1977.

[8] Patrick J. Hancock, “Design and Optimization of a High Brightness Linear UV Flashlamp and Driver Circuit For Use In Disinfection of Surfaces.” 2001. University of Missouri-Columbia. MSEE Thesis.

[9] M.A. Gusinow, "Effective blackbody temperature of high-current gas filled flashlamps," *Journal of Applied Physics*, vol. 44, pp. 4567-4568, Oct, 1973

[10] J.H.Goncz and P.B. Newell, "Spectra of Pulsed and Continuous Xenon Discharges," *Journal Of The Optical Society Of America*, vol. 56, pp. 87-92, Jun 29, 1965.

[11] M.A. Gusinow, "Spectral efficiency of pulsed high-current flashlamps," *Journal of Applied Physics*, vol. 46, pp. 4847-4851, Jun 9, 1975.

[12] J.R. Lyman Spitzer. *Physics of Fully Ionized Gases.* New York: Interscience Publishers, Inc., 1956.

[13] J.B. Bender, “Photolytic oxidation of contaminated water using the RipTide water purification system.” Anonymous 1999. Pulsar Environmental Remediation Technologies, Inc.